Percolating Conduction in Finite Nanotube Networks

S. Kumar,[1] J. Y. Murthy,[1] and M. A. Alam[2]

[1]*Department of Mechanical Engineering, Purdue University, West Lafayette, Indiana 47907-2088, USA*
[2]*School of Electrical and Computer Engineering, Purdue University, West Lafayette, Indiana 47907-1285, USA*

(Received 8 February 2005; published 1 August 2005)

The percolating conductance of a new class of nanocomposite thin-film transistors, with channels composed of isotropic ensembles of nanotubes or nanowires, is analyzed as a function of wire/tube density and channel length. The conductance exponents are validated against analytical results for short channel transistors, and against available experimental data for longer channel devices. Our plots of conductance exponents as a function of tube-to-tube coupling strength provide a unified framework to interpret future experiments and should help design better nanocomposite transistors.

DOI: 10.1103/PhysRevLett.95.066802 PACS numbers: 85.35.Kt, 73.63.Fg, 85.30.De

In recent years, there has been growing interest in low-cost large-area manufacture of thin-film transistors (TFTs) on flexible substrates such as plastic for use in applications such as displays, e-paper, e-clothing, biological and chemical sensing, conformal radar, and others [1–4]. When transistor performance is not critical, TFTs based on amorphous silicon or organics are viable [5–11]. For high performance applications, however, the choices are limited: single crystal silicon or poly-silicon based TFTs [12,13] cannot be manufactured at low temperature ($< 200°C$) and are therefore not suitable for plastic substrates. As a result, researchers are exploring a new class of nanocomposite TFTs based on bundles of silicon nanowires (Si-NWs) or carbon nanotubes (CNTs) [1,14,15]. Here, high-quality, nearly crystalline NWs and CNTs are grown at high temperature on a temporary substrate, released into a carrier fluid, and, finally spin-coated onto arbitrary (flexible) substrates at room temperature to form a thin film of randomly oriented NWs or CNTs. This thin film constitutes the high performance channel of a TFT [see Fig. 1(a)].

There is little in the literature that provides an analytical framework for understanding, controlling, and designing nanowire and nanotube composites suitable for TFTs. Results from classical percolation theory [16–19] and the geometry of Poisson tessellation [20,21] are relevant only for infinite samples with perfect tube-to-tube coupling, and are not applicable to the finite channel lengths found in TFTs. The objective of this Letter is to create a framework for the analysis of finite-sized 2D percolating networks accounting for both ballistic and diffusive transport limits, and finite intertube coupling conductance. We discuss a general framework that would apply to both tubes and wires. The analysis is used to predict the conductance of the nanotube network as a function of wire/tube densities and channel lengths. This framework may then be used to deduce the I-V characteristics of network transistors and to predict the transport properties of composites based on nanoelements of varying geometrical shapes and sizes.

In the present analysis, we consider a 2D percolating random network of nanotubes/nanowires of length L_S and diameter d randomly dispersed in a rectangular domain, as shown in Fig. 1(a) [22]. The channel length is L_C. The domain is assumed to be of height H, and the top and bottom boundaries are assumed periodic. We analyze the

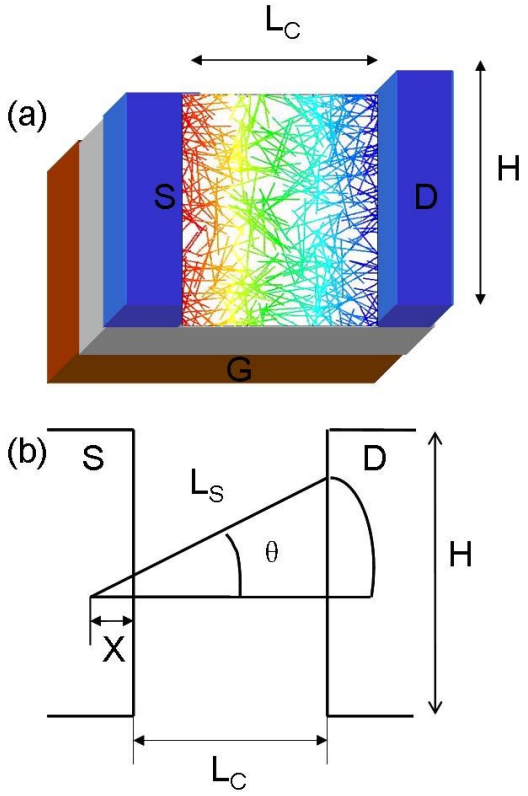

FIG. 1 (color online). (a) A thin-film network transistor with channel length L_C, channel width H, and individual tube length L_S. Source (S), drain (D), and gate (G) are also indicated; the color code of the network reflects the typical potential distribution in a nanotube network for a channel with $L_C = 3\ \mu$m, $H = 4\ \mu$m, $L_S = 2\ \mu$m, $c_{ij} = 5.0$, and $\rho = 3.5\ \mu\text{m}^{-2}$. (b) Nomenclature for bridging tube calculation.

geometry-dependent conductance properties of this network for densities below, at, or above the percolation threshold. Transport through the insulating gate substrate is assumed negligible. For transport in the tube, we consider both the ballistic limit, valid for channel lengths shorter than or comparable to mean-free-path [4,23], as well as diffusive transport, valid for long channel lengths or when substantial scattering with tube boundaries, tube-tube contacts, and with other carriers, is present. The strength of tube-to-tube contact is allowed to vary from noninteracting to perfectly contacting.

Transport in the ballistic limit.—If the channel length L_C is much shorter than the mean free path and if the tube density is below the percolation threshold, i.e., $\rho < \rho_{\text{th}} \sim 1/{L_S}^2$ (indicating low probability of tube-to-tube interaction), one may assume ballistic transport through the tubes. In this limit, in the absence of tube-tube contact, transport is independent of channel length and directly proportional to the number of tubes N_S bridging source and drain. Referring to Fig. 1(b), the angle made by a tube generated at a distance X, from the source (or drain) is $\theta = \cos^{-1}(L_C + X)/L_S$ with the maximum angle being $\theta_L = \cos^{-1}L_C/L_S$. Assuming a uniform probability for tube origination at all locations, the number of tubes making an angle between θ and $\theta + d\theta$ is given by $dN_S(\theta) = (D_x X)d\theta/(\pi/2) = (2D_x/\pi)(L_S\cos\theta - L_C)d\theta$, where D_x is the linear density of tube generation. For noninteracting tubes, the network current in the ballistic limit I_B is proportional to N_S and is given by

$$I_B \alpha N_S = \frac{2D_x}{\pi}\int_0^{\theta_L}(L_S\cos\theta - L_C)d\theta = \left(\frac{2}{\pi}\right)D_x L_S\left[\sqrt{1-\left(\frac{L_C}{L_S}\right)^2} - \left(\frac{L_C}{L_S}\right)\cos^{-1}\left(\frac{L_C}{L_S}\right)\right]. \quad (1)$$

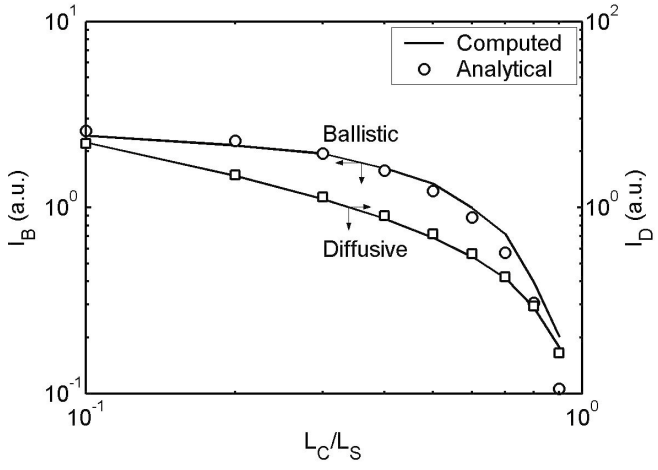

FIG. 2. Comparison of analytical results and numerical predictions of channel length dependence of ballistic and diffusive currents for densities below the percolation limit.

Figure 2 compares the value of N_S from Eq. (1) with that from our numerical network generation procedure [22] for L_C/L_S in the range 0.1–1.0. A total of 100 realizations is used in the numerical calculation. The comparison is good. As the channel length becomes comparable to or longer than the tube length, I_B is seen to go to zero; in the absence of tube-tube contact, current can only flow through the circuit if the tubes bridge source and drain. This ballistic-limit result would be realized in practice for short tube lengths with poor tube-tube contact or for tube densities below the percolation threshold where tube-tube contact would be infrequent.

Transport in the diffusive limit.—In the limit when L_C is much larger than the mean free path for electrons scattering with phonons, surface roughness, and at tube-tube contacts (at low voltage, the mean free path is defined by acoustic phonons and is typically 0.3–2 μm) [4], diffusive transport in the tube may be assumed. This limit is likely to prevail either for (a) relatively long channel transistors even with tube densities below the percolation threshold or (b) relatively short channel devices with tube densities higher than the percolation threshold, when tube-tube contact is significant. In this limit, we use drift-diffusion theory based on Kirchoff's law (instead of the classical resistor network typically used in percolation calculations) to account for imperfect tube-tube contact [17–20]. Using the continuity equation $dJ/ds = 0$ and linear response formula, $J = q\mu n\frac{d\phi}{ds}$ [24], one finds the equation for dimensionless potential distribution ϕ_i along tube i, i.e., $\frac{d^2\phi_i}{ds^2} - c_{ij}(\phi_i - \phi_j) = 0$ where s is the length along the tube (normalized to grid spacing) and $c_{ij} = G_0/G_1$, where G_0 and G_1 are the mutual and self conductances of the tubes, respectively. The quantity c_{ij} is the dimensionless charge-transfer coefficient between tubes i and j at their intersection point and is specified *a priori*; it is nonzero only at the point of intersection. Boundary conditions $\phi_i = 1$ and $\phi_i = 0$ are applied at the two ends of each tube contained in the channel region. The problem is solved numerically using the finite volume method [25].

In the long-channel noninteracting limit ($c_{ij} = 0$) below the percolation threshold, I_D is directly proportional to the number of bridging tubes, but inversely proportional to the tube length contained in the channel, so that

$$I_D \propto \frac{N_S}{W} = \left(\frac{2}{\pi}\right)D_x L_S\left[\cos^{-1}\left(\frac{L_C}{L_S}\right) - \left(\frac{L_C}{L_S}\right)\sqrt{1-\left(\frac{L_C}{L_S}\right)^2}\right] \quad (2)$$

where W is $[\sum_{i=1}^{N_S} 1/L_i]^{-1}$ [26]. The network current is also proportional to the network conductance G. Figure 2 shows a comparison of the analytical result obtained using Eq. (2) with that computed numerically using the finite volume method using 100 random realizations of the network for the case $L_C = 3$ μm, $H = 4$ μm, $c_{ij} = 0.0$, and $\rho = 5.0$ μm^{-2}. The analytical and numerical results are in

good agreement with each other, confirming the validity of our approach. As in the ballistic case, when the channel length becomes comparable to or longer than the tube length, I_D is seen to go to zero; in the absence of tube-tube contact, current can only flow through the circuit if the tubes bridge source and drain.

For the interacting case (c_{ij} nonzero) in the diffuse limit, the conductance of the finite-sized percolating network must be computed numerically using our finite volume scheme. It is computed by taking an average over 200 random realizations of the network. Comparisons are made with the experimental results reported by Snow *et al.* [15], assuming an average tube length of 2 μm. (We checked the sensitivity of our results to various probability distributions of tubes confined to 1 to 3 μm as reported in [15]. We find less than 10% variation in absolute conductance, which is well within the experimental-error margin). The percolation threshold for the network is estimated as the density at which the average distance between nanotubes equals the average length of the tube ($\rho_{\text{th}} \sim 1/\langle L_S \rangle^2 \sim 0.25\ \mu\text{m}^{-2}$). In the present context, the percolation threshold corresponds to the critical density of tubes beyond which there exists a continuous electrical path from source to drain. Simulations are performed for densities in the range 1–10 μm^{-2} for channel lengths varying from 1 to 25 μm and with a width H of 90 μm. These device dimensions and tube lengths are chosen to match those from the experiments of Snow *et al.* [15].

In Fig. 3(a), the diffuse-limit conductance σ is shown as a function of L_C/L_S for several tube densities above the percolation threshold. For these cases, we use $c_{ij} \sim 50$ based on values reported in the literature for typical CNT tube-tube contact [15,27] and mobilities [15]. For long channels ($L_S < L_C$) there are no tubes directly bridging the source and drain and current can only flow because of the presence of the network. If the tube density is sufficiently high (greater than the percolation threshold), a continuous electrical path exists from source to drain, and σ is seen to be nonzero even for $L_C/L_S > 1$. Figure 3(b) shows that the conductance exponent, n, is close to -1.0, which corresponds to ohmic conduction, for the high densities ($\rho = 10\ \mu\text{m}^{-2}$; $\rho/\rho_{\text{th}} = 40$). The exponent increases to -1.80 at lower density ($1.35\ \mu\text{m}^{-2}$; $\rho/\rho_{\text{th}} = 5$), indicating a nonlinear dependence of conductance on channel length. Note that the asymptotic limit of the conductance exponent for infinite samples with perfect tube/tube contact is -1.97 [17,18]. The linear scaling of conductance with L_C for high densities agrees very well with the experimental observations of Snow *et al.* [15]. The observed nonlinear behavior for low density is expected because the density value is close to the percolation threshold. Snow *et al.* reported a conductance exponent of -1.80 for a density of 1.0 μm^{-2} and channel length >5 μm. This value is close to that obtained from our simulations for a density of 1.35 μm^{-2}. Small variations in experimental parameters such as tube diameter, nanotube contact strength, tube electronic properties, as well as the presence of a distribution of tube lengths (1–3 μm), which is not included in the specific simulation, may explain the difference. The contact resistance between the nanotubes and the source and drain electrodes as well as insufficiently large samples for ensemble averaging in the experimental setup may also be responsible. Some evidence of this is visible in the scatter in the experimental data at low densities. *Regardless, the close correspondence of the numerical simulation and experimental measurements provide the first direct proof that the behavior of nanotube/nanowire networks in thin-film transistors and nanosensors, regardless of the visual complexity, can be understood simply as a consequence of the mathematical properties of the finite-sized tube percolation network with variable intertube coupling.*

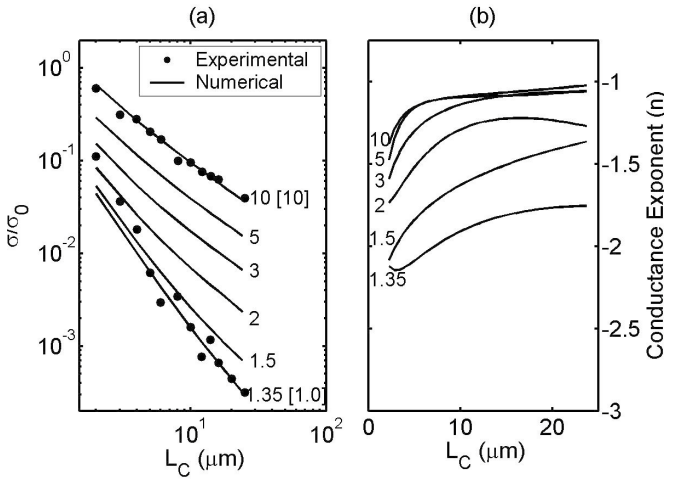

FIG. 3. (a) Computed conductance dependence on channel length for different densities (ρ) in the strong coupling limit ($c_{ij} = 50$) is compared with experimental results from [15]. $\sigma_0 = 1.0$ (simulation; $\rho = 1.35$–$10\ \mu\text{m}^{-2}$), $\sigma_0 = 1.0$ (experiment; $\rho = 1.0\ \mu\text{m}^{-2}$), and $\sigma_0 = 1.4$ (experiment; $\rho = 10.0\ \mu\text{m}^{-2}$). The number after each curve corresponds to ρ and the number in [] corresponds to ρ in experiments from [15]. (b) Dependence of the conductance exponent (n) on channel length for different densities (ρ) based on Fig. 3(a) (i.e., $\sigma/\sigma_0 \sim L_C^n$). Assumed parameters, chosen to reflect experimental conditions in [15], are: $H = 90\ \mu$m, $L_S = 2\ \mu$m, and $L_C = 1$–$25\ \mu$m.

The dependence of the conductance exponent on the channel length is explored in Fig. 3(b) for $c_{ij} \sim 50$ and for densities in the range 1.35–10 μm^{-2}, corresponding to (ρ/ρ_{th}) values of 5–40. For densities $>3.0\ \mu\text{m}^{-2}$ ($\rho/\rho_{\text{th}} > 12$), the exponent approaches -1.0 with increasing channel length (the ohmic limit). Larger exponents, corresponding to nonohmic transport, are observed for the shorter channel lengths. This is consistent with experimental observations, where conductance is seen to scale more rapidly with channel length for small L_C [15].

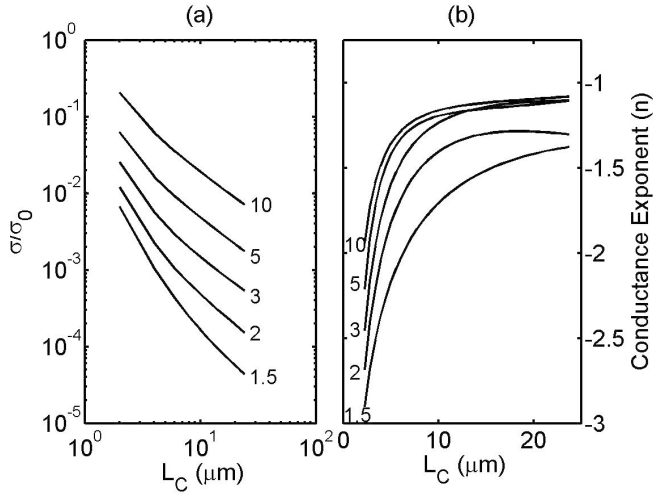

FIG. 4. (a) Computed conductance dependence on channel length for different densities (ρ) in the weak coupling limit ($c_{ij} = 10^{-3}$). (b) Corresponding conductance exponent dependence (n) on channel length for different densities (ρ). Assumed parameters are: $H = 90$ μm, $L_S = 2$ μm, and $L_C = 1$–25 μm. In (b), solid lines indicate a curve fit to the conductance exponents computed at different channel lengths using ensemble averages of numerical computations.

An important parameter governing the conductance and its exponent for the channels is the strength of tube-to-tube contact, c_{ij}. The higher value of c_{ij} (i.e., $G_0 > G_1$) represents nearly perfect contact among single-wall nanotubes (SWNTs) [15,27], while a relatively low c_{ij} value (i.e., $G_0 < G_1$) may represent interwire coupling of silicon NWs. The effect of contact conductance is explored by computing channel conductance and conductance exponents for $c_{ij} \sim 10^{-3}$, Fig. 4, and comparing the results with $c_{ij} \sim 50$, Fig. 3. The conductance drops by an order of magnitude, when c_{ij} is reduced from 50 to 10^{-3}, Fig. 4(a). For densities >3.0 μm^{-2} ($\rho/\rho_{\text{th}} > 12$), the exponent approaches -1.0 with increasing channel length for $c_{ij} \sim 10^{-3}$ similar to what is observed with $c_{ij} \sim 50$ in Fig. 4(b). For short channel lengths, a lower c_{ij} is reflected in higher conductance exponents of the sample. The contour plots in Figs. 3 and 4 can be used to put future measurements of SWNT or Si-NW based nanocomposites in perspective and can be used as independent confirmation of the density estimates. Moreover, such maps can be useful for transistor design with specific performance requirements as a function of channel length.

In summary, a computational diffusive-transport model is developed to explore the dependence of conductance on channel length for thin films made of random percolating nanotubes. The numerical results are validated against analytical solutions for noncontacting tubes in the ballistic and diffuse limits. For finite networks with tube-to-tube contact, such as those occurring at medium channel lengths ($L_C/L_S \sim 1$–10), no analytical solutions are possible. Here numerical solutions of the potential equation using Kirchoff's law for the network yield good matches with experiment. The present framework for computing conductance for medium channel lengths may prove useful in the analysis, design, and development of TFTs and in other applications of nanowire and nanotube networks.

[1] E. Menard *et al.*, Appl. Phys. Lett. **84**, 5398 (2004).
[2] E. S. Snow *et al.*, J. Vac. Sci. Technol. B **22**, 1990 (2004).
[3] W. Liang *et al.*, Nature (London) **411**, 665 (2001).
[4] A. Javey *et al.*, Phys. Rev. Lett. **92**, 106804 (2004).
[5] C. R. Kagan and P. Andry, *Thin Film Transistors* (Marcel Dekker, New York, 2003).
[6] *Technology and Applications of Amorphous Silicon*, edited by O. Madelung (Springer, Berlin, 2000).
[7] C. D. Dimitrakopoulos and D. J. Mascaro, IBM J. Res. Dev. **45**, 11 (2001).
[8] A. Curioni and W. Andreoni, IBM J. Res. Dev. **45**, 101 (2001).
[9] R. Wisnieff, Nature (London) **394**, 225 (1998).
[10] M. Pope and C. E. Swenberg, *Electronic Proceses in Organic Crystals and Polymers* (Oxford University, New York, 1999), 2nd ed., p. 337.
[11] P. Peumans, A. Yakimov, and S. R. Forrest, J. Appl. Phys. **93**, 3693 (2003).
[12] T. Tamura *et al.*, in Mater. Res. Soc. Symp. Proc. **621**, Q9.5.1 (2000).
[13] S. Uchikoga, MRS Bull. **27**, 881 (2002).
[14] X. Duan *et al.*, Nature (London) **425**, 274 (2003).
[15] E. S. Snow *et al.*, Appl. Phys. Lett. **82**, 2145 (2003).
[16] M. Stadermann *et al.*, Phys. Rev. B **69**, 201402(R) (2004).
[17] C. J. Lobb and D. J. Frank, Phy. Rev. B **30**, R4090 (1984).
[18] D. J. Frank and C. J. Lobb, Phy. Rev. B **37**, 302 (1988).
[19] D. Stauffer and A. Aharony, *Introduction to Percolation Theory* (Taylor & Francis, London, 1992).
[20] S. Goudsmith, Rev. Mod. Phys. **17**, 321 (1945).
[21] R. E. Miles, Proc. Natl. Acad. Sci. U.S.A. **52**, 901 (1964).
[22] Methodology of network generation: The source, drain, and channel regions in Fig. 1 are divided into finite rectangular control volumes. A nanotube of random orientation is originated from the control volume if a randomly generated number is less than a fixed probability p. Tubes crossing the top and bottom boundaries are treated assuming translational periodicity: that part of a tube crossing one of these boundaries reappears on the other side. The analysis is conducted only on the tubes that lie in the channel region.
[23] M. S. Lundstrom, IEEE Electron Device Lett. **18**, 361 (1997).
[24] R. F. Pierret, *Semiconductor Device Fundamentals* (Addison-Wesley, New York, 1996).
[25] S. V. Patankar, *Numerical Heat Transfer and Fluid Flow* (Hemisphere, New York, 1980).
[26] N. Pimparkar and M. Alam (unpublished).
[27] M. S. Fuhrer *et al.*, Science **288**, 494 (2000).